

## Thermodynamic Studies of Solid Polyethers

### IV. Poly(octamethylene oxide), $-\text{[(CH}_2\text{)}_8\text{O]}_n-$

Shohei YOSHIDA,\* Hiroshi SUGA, and Syûzô SEKI

*Department of Chemistry, Faculty of Science,  
Osaka University, Toyonaka, Osaka, Japan.*

(Received November 13, 1972)

**ABSTRACT:** The heat capacity of poly(octamethylene oxide) was measured in the temperature region between 13 and 360°K by using an adiabatic calorimeter. The following thermodynamic quantities were determined:  $T_g=247^\circ\text{K}$ ,  $T_m=347\pm 1^\circ\text{K}$ , and  $\Delta H_m=26.6\text{ kJ/mol}$  for sample-I,  $T_g=260^\circ\text{K}$  and  $T_m=345\pm 1^\circ\text{K}$  for sample-II, and  $T_g=255^\circ\text{K}$  for sample-III. Heat-capacity data were analysed based on Tarasov's model. Characteristic temperatures  $\theta_1$  and  $\theta_3$  were evaluated to be 550 and 116°K respectively. Heat capacities of several kinds of polyethers and their vibrational spectra obtained by an analysis based on Tarasov's model were compared with each other.

**KEY WORDS** Poly(octamethylene oxide) / Heat Capacity / Glass Transition / Tarasov's Model / Polyethers / Vibrational Spectra /

In the preceding papers,<sup>3,4</sup> we have reported the results of a series of thermodynamic studies for some polyethers. In the present investigation, we studied the thermodynamic properties of poly(octamethylene oxide) (abbreviated as POMO hereafter).

Tadokoro, *et al.*,<sup>1</sup> determined the crystal structure of POMO by use of the X-ray diffraction method. According to their results, there are two modifications, Polyethylene(PE)- and Polytetrahydrofuran(PTHF)-types, named by them, in the crystalline part of POMO. The chain conformation is planar zigzag in both crystalline forms, even though the direction of plane of the planar zigzag in the crystallographic unit cell is different. PE-type is formed almost always with the same amount of PTHF-type, from its methanolic solution. However, by cooling the melt we can obtain almost pure PTHF-type crystals. The crystal structure of PE-type is orthorhombic,  $z=2$ , while PTHF-type has the monoclinic structure with  $z=2$ .

In order to clarify the thermodynamic properties of these states, we measured the heat capacity of three kinds of samples, of which one was made from its methanolic solution and the other two from the melt; each was subjected to dif-

ferent thermal treatments. Heat capacity data thus obtained was analysed by using Tarasov's model,<sup>2</sup> as was done for other polyethers.<sup>4</sup>

In the preceding papers, we compared the thermodynamic properties such as temperature, enthalpy, and entropy of melting,<sup>3</sup> and glass transition temperature.<sup>4</sup> The thermodynamic values for melting were found to vary systematically, while the glass transition temperatures did not. In this paper, we compare and examine the heat capacities of polyethers and the results of an analysis based on Tarasov's model.<sup>2</sup>

## EXPERIMENTAL

### *Preparation of POMO*

The monomer, a commercial sample (Nakarai Chemicals) of *n*-octamethylene glycol, was purified by repeated crystallization from a solution of acetone—ether mixture (2:3 in weight ratio). Polymerization was carried out in a reaction tube which was designed following the suggestions by Rhoad and Flory.<sup>5</sup> After 40g of the purified monomer sample and small amounts of concentrated sulfuric acid and  $(\text{C}_2\text{H}_5)_2\text{OBF}_3$  (Nakarai Chemicals) had been introduced into the tube, it was evacuated for degassing. Then the mixture was heated up and polymerized in the temperature region from 160 to 210°C under

\* Present Address: *Ashigara Research Laboratory, Fuji Photo Film, Co., Minamishigara, Kanagawa.*

a constant stream of dry nitrogen gas. The product was dissolved into hot methanol (*ca.* 50°C) and then precipitated by cooling the solution down to room temperature. It was further purified by repeated precipitation from benzene solution with methanol. Finally, it was dried in vacuum ( $10^{-5}$  mmHg) at 30 to 50°C for a week.

Infrared spectra of this sample were taken for identification, using the data of Tadokoro, *et al.*<sup>1</sup> The sample was also characterized by measuring the viscosity of its benzene solution at 30°C. Based on these results, the average molecular weight was estimated to be about 7000, using the data for polyhexamethylen oxide and polydecamethylene oxide of Fujita, *et al.*<sup>6</sup>

As was described in the previous section, there are two known crystalline forms for POMO. Therefore, X-ray diffraction spectra were measured in order to identify the crystalline form and also to examine the thermodynamic stability of the sample (see below). Figure 1(A), shows the X-ray diffraction spectrum obtained for the sample precipitated from its methanolic solution at 70°C with a cooling rate of 0.1°K/hr, while the spectrum for the sample crystallized from the melt is shown in Figure 1(B). According to these results, the crystalline part of the sample

precipitated from its methanolic solution with the slow cooling rate was confirmed to be a mixture of the crystalline forms of PE- and PTHF-types. The weight ratio of PE- and PTHF-types in this sample was estimated to be 6 to 4. On the other hand, the sample crystallized from the melt consisted almost completely of the crystalline form of PTHF-types. After these samples were preserved at room temperature for a month or so, the X-ray diffraction spectra were taken again and it was confirmed that the crystalline form of the samples remained unchanged at least at room temperature.

#### Measurement of Heat Capacity

Prior to the precise measurement of heat capacity, thermal behavior was investigated by using DSC (Perkin-Elmer Model 1B).

The calorimeter used in this study was an adiabatic calorimeter which was designed to measure the heat capacity of solid or liquid samples in the temperature region from 11 to 360°K. The thermometers used were platinum-resistance thermometers manufactured by Tinsley Co. The sample container was made of gold (18K), with a capacity of about 30 cm<sup>3</sup>. The container with sample was sealed by Rose's alloy under a dried nitrogen atmosphere and evacuated for about 24 hr through the capillary tube attached to the container; helium gas (200 mmHg) was then introduced into the container for reaching thermal equilibration as quickly as possible.

The heat capacity was measured for these three samples prepared by different methods. One of them (sample-I) was precipitated from its methanol solution by slow cooling. Samples-II and -III were made from the melt and then subjected to an annealing and rapid cooling treatments respectively. These thermal treatments were carried out in the container by procedures similar to those for PTHF.<sup>4</sup> The measurement of the heat capacity was performed by means of the intermittent heating technique, but in the region of melting the continuous heating technique was employed. The heating rate was 3 to 7°K/hr. The measurement covered the temperature region from 13 to 360°K.

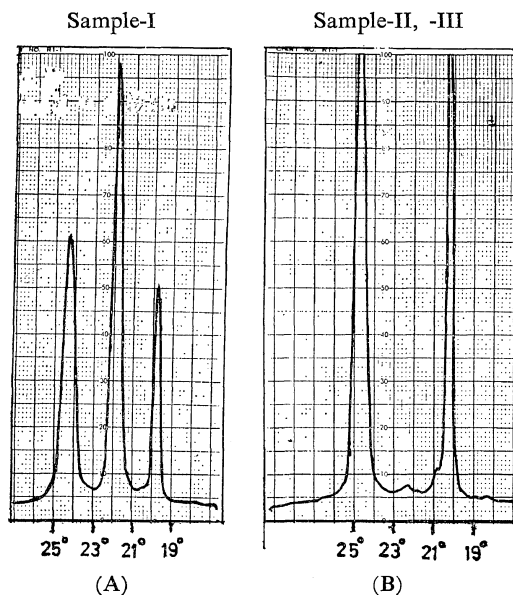


Figure 1. X-ray diffraction spectra.

## RESULTS AND DISCUSSION

*Heat-Capacity Data*

The DSC curves obtained are shown in Figure 2. The sample-I showed three peaks between 335 and 343°K. On the other hand, the sample crystallized from the melt showed a single peak around 340°K. These peaks were affected by the annealing procedure. For the appearance of three peaks in the DSC curve for sample-I two possible origins will be considered. One will be the usual occurrence of multiple melting peaks in a solid high polymer, which may reflect texture, such as folded chain structure, etc. The other possible origin is the fact that, as was mentioned in the previous section, this sample is a mixture of crystals of PE- and PTHF-types. In order to clarify this point, simultaneous measurements of X-ray diffraction, electroscopic examination, and calorimetry around the melting region will be required.

The heat capacities obtained are shown in Figure 3 and are given in Tables I, II, and III. The heat capacity values of the three kinds of samples did not show any remarkable difference below 200°K, but above this temperature they

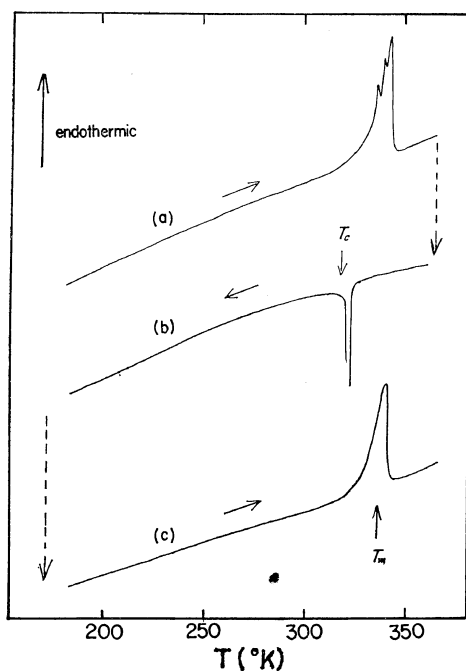


Figure 2. DSC curves of POMO: (a), sample-I.

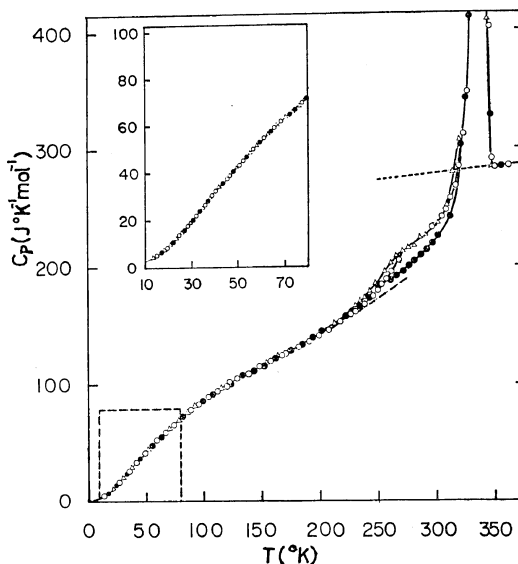


Figure 3. Heat capacity of POMO: ●, sample-I; ○, sample-II; △, sample-III.

showed evident differences. The glass transition temperature was found to be 247, 260, and 255°K for the samples-I, -II, and -III, respectively. The melting temperature was found to be  $347 \pm 1$  and  $345 \pm 1$ °K for the samples-I and -II respectively. The crystallinity was also evaluated to be 91 and 73% for samples-I and -II by the same procedure used for PTHF.<sup>4</sup> Heat of fusion was evaluated to be 26.6 kJ/mol for sample-I. As for the completely crystalline state, heat and entropy of fusion were estimated to be 29.3 kJ/mol and 84.4 J/°K mol respectively. Here the entropy of fusion is the value corresponding to the value of the lower limit. The heat of fusion for sample-II was evaluated to be 21.3 kJ/mol.

The heat capacity of sample-I approximately coincided with that of sample-II in the low temperature region, in spite of the considerable difference in their crystallinities. This fact may indicate that there is some difference between the heat capacities of the crystalline states of PE- and PTHF-types in the low temperature region. Arguing from the conditions of preparation, the crystal of PE-type might be more thermodynamically stable than that of PTHF-type. However, it is not clear at this stage of the present investigation whether the PE-type or the PTHF-type of crystalline state is more thermodynamically stable.

Table I. Heat capacity of POMO (sample-I)

$T$ K	$C_p$ JK <sup>-1</sup> mol <sup>-1</sup>	$T$ K	$C_p$ JK <sup>-1</sup> mol <sup>-1</sup>
13.66	5.091	165.43	124.7
14.87	5.430	170.01	126.7
15.93	5.872	174.54	129.5
16.85	6.430	179.03	131.3
17.68	7.106	184.42	134.2
18.44	7.595	188.77	136.5
19.14	8.276	193.06	139.8
19.85	9.004	197.34	141.7
20.64	9.72	201.64	144.6
21.57	10.92	206.06	146.9
22.97	11.91	210.42	149.7
24.72	13.66	214.60	152.4
26.73	15.88	218.74	154.9
29.00	18.85	222.90	158.0
31.17	21.02	227.16	161.8
33.12	23.49	230.73	164.3
34.96	25.22	234.26	166.6
36.79	27.49	238.47	169.7
38.49	29.66	242.64	173.5
40.24	31.35	250.92	182.9
42.07	33.42	254.97	185.1
44.27	35.95	260.36	188.7
46.82	38.80	266.35	192.5
49.20	42.00	271.61	195.8
51.45	44.02	276.80	200.1
54.10	47.44	281.91	204.7
57.23	50.30	286.95	209.3
60.70	53.96	291.91	214.0
64.38	57.55	296.79	219.4
67.88	60.45	301.68	225.4
71.90	64.43	311.58	242.5
75.85	67.88	321.03	302.3
79.62	71.59	325.40	343.5
91.45	80.80	329.32	412.3
103.74	89.26	332.50	652.8
108.97	92.30	334.65	1140.7
114.07	95.55	336.13	1709.9
119.05	98.50	337.31	2421.4
123.94	101.3	338.46	2199.4
128.74	104.0	339.58	2224.6
133.42	106.7	340.26	2506.7
138.02	109.6	340.81	2585.4
142.54	111.6	341.43	3736.8
147.00	114.5	342.16	4607.8
151.46	116.5	344.40	864.9
156.09	119.3	347.31	328.2
160.80	122.0	357.2	284.8

Table II. Heat capacity of POMO (sample-II)

$T$ K	$C_p$ JK <sup>-1</sup> mol <sup>-1</sup>	$T$ K	$C_p$ JK <sup>-1</sup> mol <sup>-1</sup>
13.74	4.637	157.83	120.0
14.91	4.901	162.63	122.6
15.96	5.772	167.35	125.0
16.90	6.408	172.02	127.7
17.75	7.221	176.62	130.1
18.54	7.806	181.21	132.0
19.29	8.612	185.75	134.3
20.05	9.192	190.20	136.2
20.84	9.869	194.60	139.5
21.72	10.88	198.95	141.2
22.98	12.53	203.25	143.6
24.76	13.85	207.51	146.0
26.95	16.11	211.72	148.9
31.35	21.15	217.57	153.7
33.22	23.30	221.66	155.3
35.04	25.78	226.26	159.4
36.96	28.07	230.24	162.2
38.87	30.51	234.17	165.6
40.70	32.06	238.06	167.9
42.50	34.62	241.89	172.3
44.47	36.48	245.67	174.4
46.63	38.85	249.40	179.7
48.82	41.39	253.19	184.1
51.66	44.48	257.19	189.3
55.24	48.39	269.94	206.4
58.84	52.71	274.91	214.4
62.21	56.11	279.27	219.7
65.40	59.22	283.59	221.5
76.80	68.94	292.08	228.9
84.40	75.58	296.25	232.3
88.83	79.36	304.49	241.3
92.76	81.91	308.50	247.1
96.59	84.60	312.42	256.9
100.33	87.64	316.24	267.4
104.01	90.10	319.92	284.4
107.59	92.36	323.64	311.1
111.94	94.96	327.56	347.1
117.04	98.06	334.08	607.3
122.09	100.2	336.88	1007.7
129.19	104.8	339.06	1996.4
133.97	107.8	345.94	402.1
138.67	110.4	347.61	290.8
143.28	112.8	350.43	283.2
148.05	115.9	353.47	285.2
152.98	117.4		

**Table III.** Heat capacity of POMO (sample-III)

$T$ K	$C_p$ JK <sup>-1</sup> mol <sup>-1</sup>	$T$ K	$C_p$ JK <sup>-1</sup> mol <sup>-1</sup>
13.54	4.579	142.80	112.7
14.52	5.080	148.22	115.7
15.43	5.589	153.55	118.6
16.37	6.305	158.80	121.0
17.36	7.128	163.97	124.0
18.31	7.993	169.07	126.3
19.22	8.876	175.09	130.4
20.16	9.974	180.03	132.8
21.13	10.74	184.91	135.2
22.10	11.61	189.72	137.9
23.12	12.50	194.46	140.4
24.30	13.80	199.16	142.7
25.79	15.42	203.79	145.9
27.79	17.64	208.38	148.7
30.05	20.01	212.91	151.9
32.28	22.53	217.40	155.1
34.38	25.28	221.81	158.9
36.34	27.31	226.19	163.1
38.41	29.82	230.50	166.4
40.53	32.32	234.75	170.2
42.54	34.50	238.94	173.9
44.57	37.29	243.08	179.0
46.69	39.63	248.42	185.3
48.85	41.65	256.38	195.7
51.43	44.42	261.04	202.5
54.62	48.28	266.18	208.4
58.39	52.12	271.30	212.2
62.44	56.28	276.27	215.2
66.23	59.61	281.30	216.6
70.23	63.27	286.36	224.8
74.43	66.90	291.36	225.8
78.44	70.37	296.32	230.9
86.76	77.48	301.22	236.4
92.06	81.22	309.20	250.8
97.16	84.81	314.53	279.6
102.12	88.04	320.15	306.9
107.72	92.05	326.12	358.6
113.94	95.78	331.87	540.1
119.99	99.87	344.66	409.8
131.64	106.5	348.50	283.8
137.28	109.8	352.77	284.8

#### Analysis of Heat Capacity

Due to the facts described above, it is very difficult to estimate the heat-capacity values of the completely crystalline state of each PE- and PTHF-type. Therefore the experimental heat-capacity values for sample-I were used for the calculation of heat capacity without corrections

for either the crystallinity or the ratio of coexistence of the PE- and PTHF-types of crystalline states. However, this approximation would not lead to essential errors in the calculation above 30°K. These experimental heat-capacity values were converted into heat-capacity values at constant volume by the same procedure as in the case of polyoxacyclobutane.<sup>11</sup>

For a single chain of POMO, there are 75 normal vibrational modes per chemical repeating unit, which are composed of the 8 CH<sub>2</sub> symmetry-stretching, antisymmetry-stretching, bending, wagging, twisting, and rocking modes and the 9 skeletal stretching, bending, and torsional modes. As these normal vibrations have never been analysed, the data of PTHF was substituted for the data of POMO in the calculation of its heat capacity.

The calculation was carried out by the same three trials used previously for PTHF.<sup>4</sup> The first one, where we tried to fit the contribution of all the skeletal vibrations into Tarasov's heat capacity,<sup>2</sup> was unsuccessful as these calculated values deviated more than 20% from the experimental values in several temperature regions. A good fit was obtained in the second trial where the contributions from the CH<sub>2</sub> group vibrations as well as the skeletal stretching ones

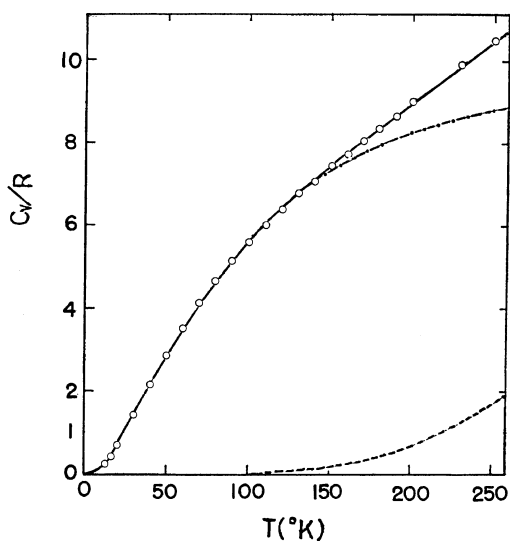


**Figure 4.** Heat capacity of POMO: ○, exptl; —, calcd (total); - - -, Tarasov approximation; - · - ·, by skeletal stretch. and CH<sub>2</sub> group vibrations.

**Table IV.** Experimental and calculated heat capacity of POMO (sample-I)

T/K	$C_v/R$ per mole repeating unit		
	experimental	calculated	deviation %
13.5	0.495	0.441	-8.8
15	0.607	0.589	-2.9
20	1.094	1.174	-7.3
30	2.377	2.497	+4.9
40	3.768	3.794	+0.5
50	5.123	5.013	-2.1
60	6.378	6.169	-3.2
70	7.514	7.259	-3.1
80	8.532	8.282	-2.9
90	9.510	9.229	-3.0
100	10.35	10.09	-2.5
110	11.08	10.88	-1.8
120	11.73	11.61	-1.0
130	12.40	12.27	-1.0
140	13.03	12.87	-1.1
150	13.56	13.48	-0.5
160	14.11	14.03	-0.4
170	14.66	14.58	-0.6
180	15.23	15.11	-0.7
190	15.75	15.66	-0.6
200	16.29	16.19	-0.6
230	18.19	17.88	-1.6
250	19.30	19.09	-1.5

were approximated by Einstein functions and the contributions by other vibrations were calculated by Tarasov's model.<sup>4</sup> The calculated heat capacity is shown in Figure 4 and given in Table IV, together with the experimental heat capacity. In this case,  $\theta_1$ ,  $\theta_3$  and  $\theta_3/\theta_1$ , where  $\theta_1$  and  $\theta_3$  were characteristic temperatures in Tarasov's model, were evaluated to be 550°K, 116°K and 0.210, respectively. Based on these results, the heat capacity of POMO is successfully reproduced by the relation:

$$C_v = 18RC_{1,3}(\theta_1, \theta_3) + 9RE(\theta_E^3) + R \sum_{48} E(\theta_E^{CH_2}),$$

(per mole of chemical repeating unit)

where  $C_{1,3}$  is Tarasov's heat capacity function with  $\theta_1=550^\circ\text{K}$  and  $\theta_3=116^\circ\text{K}$  and  $E$  the Einstein function, with  $\theta_E^3$  and  $\theta_E^{CH_2}$  the characteristic temperatures for the skeletal stretching and  $\text{CH}_2$  group vibration respectively.

In the third trial, the contribution from the one special skeletal bending mode was also treated by an Einstein function, and the remain-

der was approximated by Tarasov's model. In this case,  $\theta_1$  and  $\theta_3$  were evaluated to be 500 and 118°K respectively.

Comparing these two trials with each other, the second one was found to be better than the third one, as in the latter case the deviation between the calculated and experimental heat-capacity values amounted to more than 15% of the experimental ones in several temperature regions. These results will be compared with those of other polyethers in the next section.

#### Comparison of Heat Capacities of Polyethers

In the preceding papers,<sup>3,4</sup> the heat capacity of the crystalline state of some polyethers was analysed using Tarasov's model.<sup>2</sup> In the calculation of the heat capacity, the contributions of the vibrations in the  $\text{CH}_2$  groups and of the skeletal stretching vibrations to the heat capacity data were approximated by the Einstein function. The contributions of other vibration were approximated by two sets of trial functions.

In one trial for all samples, the contributions of these vibrational modes, which consisted of the skeletal bending and torsional vibrational modes in a single chain model, was calculated by Tarasov's model. In this case the heat capacity of Poly(oxacyclobutane) (POCB), PTHF, and POMO were successfully approximated, but for Poly(ethylene oxide) (PEO) and Poly(oxymethylene) (POM), this trial failed to explain the experimental heat capacity.

In another trial for all samples, the contribution of one of the skeletal bending vibrational modes as well as those of the vibrational modes in the  $\text{CH}_2$  group and of the skeletal stretching vibrational modes was treated by Einstein functions with separate characteristic temperatures. The contributions of the other skeletal vibrational modes were treated by using Tarasov's model. In this case the heat capacity of POM, and PEO could be successfully explained.

Figure 5 shows the schematic diagram of the frequency distribution for the skeletal vibrations, except for the skeletal stretching vibrations, of the crystalline polyethers. Thus, this figure shows the frequency distribution for the skeletal bending and torsional vibrational modes in a single chain model. In addition, the frequency distribution for PE, which was estimated by

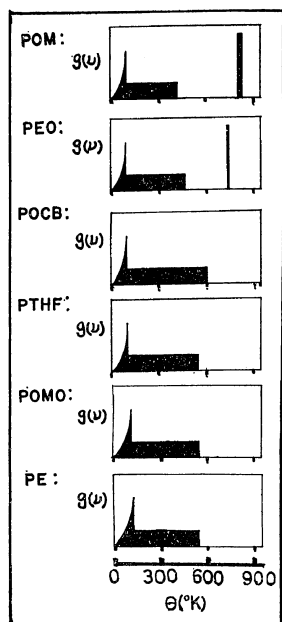


**Figure 5.** Schematic diagrams of frequency distributions of vibrations for polyethers omitting skeletal stretch and  $\text{CH}_2$  group vibrations.

Wunderlich,<sup>7</sup> is given in this figure for comparison. The horizontal scale is in temperature units in this figure; the vertical scale is arbitrary.

Comparing these frequency distributions, the  $\theta_1$  values of five substances (the characteristic temperature of the one-dimensional part in the Tarasov frequency distribution) become higher with a decreasing value of  $m$  in  $\text{-(CH}_2)_m\text{O-}$ . For PEO and POM, the frequency distribution can be expressed only by taking the Tarasov-type and Einstein-type treatments. In other words, this fact may express the tendency for the number of independent optical modes with higher frequency to increase with a decrease in  $m$  value in  $\text{-(CH}_2)_m\text{O-}$ .

Considering the results by other workers on the normal vibration analysis for POM<sup>9</sup> and PEO,<sup>10</sup> the  $\theta_1$  value may be concerned with the skeletal bending modes in a "single chain model", whereas the  $\theta_3$  value, which is the characteristic temperature of three-dimensional part in the Tarasov frequency distribution, may be affected mainly by the skeletal torsional modes in a "single chain model". Putting this physical

meaning on  $\theta_1$  and  $\theta_3$  values, the general trend given in Figure 5 may suggest that the skeletal bending modes become separated from the skeletal torsional modes in a single chain model upon lowering the  $m$  value in  $\text{-(CH}_2)_m\text{O-}$ . This behavior may reflect the fact that for POM and PEO the molecular chain conformation is helical.

Figure 6 shows the heat capacity of the completely crystalline state of POM, POCB, and PE per bead mole. Here, "bead"<sup>8</sup> means the average group constituting the chemical repeating unit: e.g., for POCB, weight of  $(\text{CH}_2\text{CH}_2\text{CH}_2\text{O})/4 =$  weight of unit bead. Above  $90^\circ\text{K}$ , the heat capacities have higher values in the order of POM, POCB, and PE, whereas below  $50^\circ\text{K}$ , this relation is inverted. As one of the origins for this behavior, the difference in the proportion of the  $\text{CH}_2$  group in the repeating unit will be considered. So, by subtracting the contribution of the  $\text{CH}_2$  group from the experimental heat capacity, the heat capacity due to the skeletal vibrations was estimated. The result thus obtained is shown in Figure 7. Although the heat capacity values above  $150^\circ\text{K}$  in this figure become lower, the relative relationship among the heat capacities of POM, POCB, and PE is substantially identical with that in Figure 6. These behaviors are consistent with those of the frequency distribution in the result of the analysis based on Tarasov's model as shown in Figure 5.

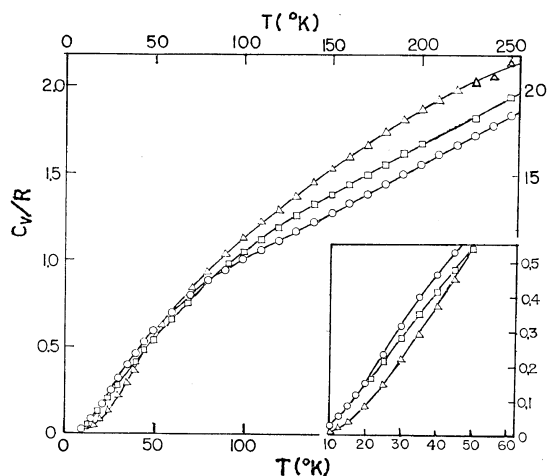


**Figure 6.** Heat capacity per one mole of "bead" of polyethers:  $\circ$ , POM;  $\square$ , POCB;  $\triangle$ , PE.

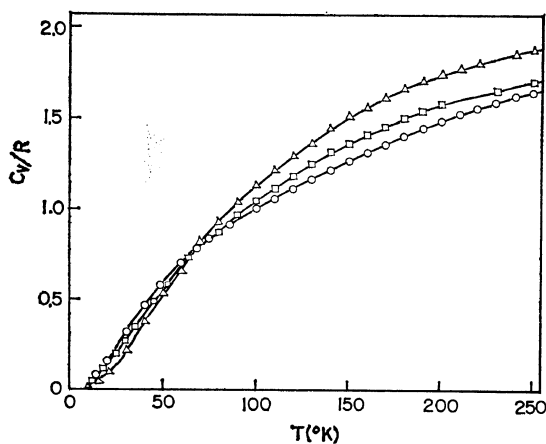


Figure 7. Heat capacity per one mole of "bead" of POM (○), POCB (□), and PE (△). The contribution of CH<sub>2</sub> group is subtracted).

*Acknowledgment.* The authors wish to express their sincere thanks to Professor H. Tadokoro, Assistant Professor Y. Chatani, and Dr. M. Kobayashi of Osaka University for the detailed information about the structural and spectroscopic data for POMO. Thanks are also due to Professor H. Fujita of Osaka University and Dr. K. Nakao of Industrial Research Institute, Osaka Prefecture for allowing the authors to use the

apparatus for molecular weight measurement and the gel permeation chromatography apparatus respectively.

#### REFERENCES

1. S. Kobayashi, H. Tadokoro, and Y. Chatani, *Makromol. Chem.*, **112**, 225 (1968).
2. V. V. Tarasov, "New Programs in the Physics of Glass" Israel Program for Scientific Translations, Jerusalem, 1963.
3. S. Yoshida, M. Sakiyama, and S. Seki, *Polymer J.* **1**, 573 (1970).
4. S. Yoshida, H. Suga and S. Seki, *ibid.*, **5**, 00 (1973).
5. M. J. Rhoad and P. J. Flory, *J. Amer. Chem. Soc.*, **72**, 2216 (1950).
6. K. Yamamoto and H. Fujita, *Polymer*, **7**, 557 (1966).
7. B. Wunderlich, *J. Chem. Phys.*, **37**, 1207 (1962); B. Wunderlich and H. Baur, *Fortsh. Hochpolym. Forsh.*, **7**, 151 (1970).
8. B. Wunderlich, *J. Phys. Chem.*, **64**, 1052 (1960).
9. L. Piseri and G. Zerbi, *ibid.*, **48**, 3561 (1968).
10. H. Matsuura and T. Miyazawa, *ibid.*, **50**, 915 (1969); *Bull. Chem. Soc. Jap.* **41**, 1768 (1968).
11. S. Yoshida, H. Suga, and S. Seki, *Polmer J.* **5**, 00 (1973).